1026 *J. Chem. Eng. Data* **2004,** *49,* 1026−1031

Densities and Solubilities for Binary Systems of Carbon Dioxide + Water and Carbon Dioxide + Brine at 59 °C and Pressures to 29 MPa

Zhaowen Li, Mingzhe Dong,* Shuliang Li, and Liming Dai

Faculty of Engineering, University of Regina, Regina, Saskatchewan, Canada S4S 0A2

Densities and solubilities for binary systems of carbon dioxide + water and carbon dioxide + Weyburn-formation brine were measured at a temperature of 59 °C and pressures up to 29 MPa. Density values were obtained for both the saturated and unsaturated aqueous carbon dioxide solutions at different pressures. A correlation in the literature was used to predict the solubility of carbon dioxide in the aqueous phase, and the results were compared with the measured data. The measured density of aqueous carbon dioxide solutions was correlated as a function of carbon dioxide concentration and pressure. A simple method for determining the density of aqueous carbon dioxide solutions was recommended.

Introduction

The increase of CO_2 concentration in the atmosphere has been considered one of the greatest factors of global warming. To mitigate the accumulation of CO_2 in the atmosphere, CO_2 capture and storage have been widely investigated since the early 1990s. The two most promising options for CO_2 storage are in depleted oil and gas reservoirs and in deep oceans. The solubility of CO_2 in aqueous solution and the density of aqueous CO_2 solution as a function of pressure are important phase behavior data required for modeling CO_2 sequestration and migration in reservoirs or oceans. In addition, these data are very useful in the simulation of CO_2-related enhanced oil recovery processes. Other applications may also be found in chemical and environmental engineering.

Different from most of the other gases, the dissolution of CO_2 in aqueous solution under most reservoir or deep-ocean conditions results in an increase in density of the solution, which can induce a natural convection. On the basis of this phenomenon, Haugan and Drange[1] proposed a CO_2 sequestration method in the deep ocean by a shallow CO_2 injection in the upper 200−400 m of the ocean. For CO_2 sequestration in depleted oil reservoirs, the density-induced natural convection needs to be investigated in order to make a better prediction of the CO_2 migration process underground. Therefore, the density data of CO_2−formation water is essential to the prediction.

Some results for the density of aqueous CO_2 solutions have been reported under deep ocean conditions: CO_2 + seawater at 3 °C and 35 MPa by Ohsumi et al.;[2] CO_2 + water at 5−20 °C and 6.44−29.49 MPa by Teng and Yamasaki[3]. Parkinson and Nevers[4] reported the densities of CO_2 + water solutions in a temperature range from 4.95 °C to 40.55 °C and pressures up to 3.4 MPa. More recently, Yaginuma et al.[5] measured the densities of CO_2 + distilled water at 31 °C and pressures up to 10 MPa. However, for the density of CO_2 + formation brine solutions under practical reservoir conditions (high pressure, elevated temperature, and various salinities) more experimental measurements are required. The solubilities of CO_2 in water or synthetic brine (NaCl and $CaCl_2$ solutions) under different conditions were reported by many researchers.[3,6−10] Recently, results of CO_2 solubility in a variety of aqueous solutions were reported.[11−14] These solutions are mainly used in the processing industry and are quite different from reservoir brines. Experimental measurements are still needed for CO_2 solubility in reservoir brine samples in order to examine the reliability of the available correlations under reservoir conditions.

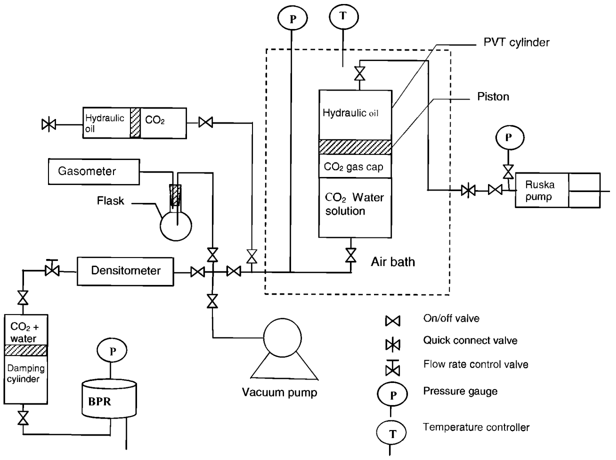

Figure 1. Schematic diagram of experimental apparatus.

This paper reports the experimental results of CO_2 solubilities in deionized water and an oil reservoir formation brine as a function of pressure and the densities of these aqueous CO_2 solutions as a function of both CO_2 concentration and pressure. The pressure covered in the measurements ranged from 0.3 MPa to 29 MPa. All measurements were made at 59 °C, the temperature of Weyburn reservoir where an International Energy Agency Weyburn CO_2 monitoring and storage project is underway.

Experimental Section

Apparatus. A schematic diagram of the experimental apparatus is shown in Figure 1. This apparatus is similar to a pressure−volume−temperature (PVT) test system. It mainly consists of a 500-cm^3 PVT cylinder, a high-pressure CO_2 cylinder, a high-pressure Ruska pump, a back pressure regulator (BPR), a densitometer, and a gasometer.

---

* To whom correspondence may be addressed. E-mail: Mingzhe.Dong@uregina.ca.

10.1021/je049945c CCC: $27.50

Table 1. Analysis of Weyburn Formation Brine Sample

density/(g·cm^{-3}) at 22 °C	1.0619
at 59 °C	1.0459
total dissolved solids/(mg·L^{-1})	92950
calcium/(mg·L^{-1})	1970
sodium/(mg·L^{-1})	29140
magnesium/(mg·L^{-1})	566
potassium/(mg·L^{-1})	454
iron/(mg·L^{-1})	<0.2
chloride/(mg·L^{-1})	52640
sulfate/(mg·L^{-1})	3800
pH at 20 °C	7.67

Table 2. Solubility of CO_2 in Deionized Water at 59 °C

	CO_2 solubility/(10^{-3} mol·cm^{-3})		
P/MPa	measured	predicted	relative error (%)
19.89	1.344	1.337	0.49
15.62	1.227	1.256	2.34
11.76	1.127	1.142	1.31
10.14	1.089	1.074	1.43
6.27	0.835	0.838	0.34
3.34	0.514	0.546	5.83

The PVT cylinder was used to equilibrate the CO_2 and the aqueous solution. It was placed in an air bath and can be rocked to speed up the equilibration between the CO_2 and the aqueous solution. The temperature of the air bath was controlled within ±0.5 °C of the desired value. The pressure of the cylinder was monitored by a Heise pressure gauge (Dresser Instrument) with an accuracy of ±0.025% of the full-scale span (34.5 MPa). The high-pressure CO_2 cylinder was used to contain the prepressurized CO_2. The Ruska pump was used to pressurize and transfer fluids. The BPR was connected to the densitometer through a damping cylinder. This was used to keep the pressure of the system constant when transferring the saturated aqueous CO_2 solutions from the PVT cylinder to the densitometer. Density was measured using a DMA 512P (Anton Paar) vibrating-tube densitometer with a repeatability of $\pm 1 \times 10^{-5}$ g·cm^{-3}. The temperature in density measurement was controlled within ±0.2 °C by the circulating oil bath. The Ruska gasometer combined with a flask was employed to determine the CO_2-to-water ratio of the solution.

Procedures. Before starting a test, approximately 450 cm^3 of water sample was introduced into the PVT cylinder. Prior to adding CO_2 into the cylinder, the density of the water sample was measured at different pressures up to 29 MPa. Then the pressure was reduced to a lower level, and CO_2 was injected. The minimum amount of CO_2 needed for a test was estimated using the Chang et al.[15] correlation. To make sure that there was a gas cap at equilibrium, 30% more CO_2 than the estimated amount was added to the PVT cylinder. After the fluids in the PVT cylinder were pressurized up to a desired pressure, the cylinder was rocked frequently to accelerate the dissolving process. When the cylinder pressure stayed constant over a period of more than 5 h, the equilibrium between the CO_2 phase and the aqueous phase was considered to be reached.

Once the equilibrium was achieved at a given pressure, about 20 cm^3 of CO_2 + water solution was transferred to the densitometer under a pressure which was 5−10 kPa higher than the saturation (or equilibrium) pressure with an assistance of the BPR. The density of CO_2 + water solution was first measured at the saturation pressure. Then the densities of the same CO_2 aqueous solution at elevated pressures were determined. These measurements gave the densities of the aqueous solution under different pressures (at and above saturation pressures) for a constant CO_2 concentration.

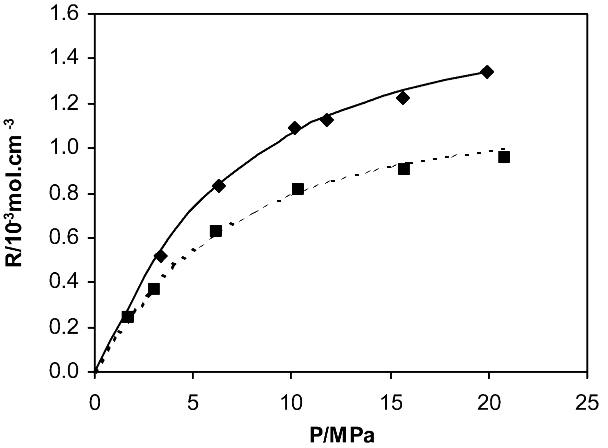

Figure 2. Solubility of CO_2, *R*, in deionized water and Weyburn brine vs pressure at 59 °C. ◆, Deionized water, measured; ■ brine, measured; solid line, deionized water, predicted; dashed line, brine, predicted.

Table 3. Solubility of CO_2 in Weyburn Brine at 59 °C

	CO_2 solubility/(10^{-3} mol·cm^{-3})		
P/MPa	measured	predicted	relative error (%)
20.87	0.958	1.002	4.37
15.72	0.905	0.934	3.10
10.38	0.814	0.805	1.09
6.20	0.626	0.618	1.32
3.01	0.367	0.374	1.83
1.76	0.240	0.239	0.18

Table 4. Values of Coefficients in Equations 4−6

	$i = 0$	$i = 1$	$i = 2$	$i = 3$	$i = 4$
a_i	1.163	−16.630	111.073	−376.859	524.889
b_i	0.965	−0.272	0.0923	−0.1008	0.0998
c_i	1.280	−10.757	52.696	−222.395	462.672

Another 20 cm^3 solution was released from the PVT cylinder to the atmospheric pressure to determine the CO_2 solubility in aqueous phase at the saturation pressure. The liquid was collected in the flask, and its mass was measured. The evolved CO_2 was collected in the gasometer, where its volume was determined at ambient conditions. The atmospheric pressure was 101.2 ± 0.1 kPa in all measurements. From the mass of the liquid and the volume of the CO_2, the solubility of CO_2 in aqueous solution at the saturation pressure and test temperature was calculated from the following equation

$$R = \frac{n_g}{(m_g + m_w)/\rho_s} \tag{1}$$

where *R* is the solubility of CO_2 in aqueous phase, n_g and m_g are the number of moles and mass of CO_2, respectively, m_w is the mass of water, and ρ_s is the density of aqueous CO_2 solution at the saturation pressure. n_g is calculated from the measured gas volume using the equation of state, and m_g is the product of n_g and the molecular weight of CO_2. It should be noted that this technique of measuring solubility of CO_2 is suitable for nearly neutral aqueous solutions, such as most reservoir brines, but may not be sufficient when the pH value of water sample is high. For the latter case, the reaction between CO_2 and the aqueous solution has to be considered.

The PVT equilibrium measurements were started from a high saturation pressure. After the first measurement, the pressure in the PVT cylinder was lowered to the next

Table 5. Densities of CO_2 + Deionized Water Solutions at 59 °C

P/MPa	ρ/(g·cm^{-3})[a]	P/MPa	ρ/(g·cm^{-3})	P/MPa	ρ/(g·cm^{-3})	P/MPa	ρ/(g·cm^{-3})	P/MPa	ρ/(g·cm^{-3})	P/MPa	ρ/(g·cm^{-3})	P/MPa	ρ/(g·cm^{-3})
		3.34	**0.9905**	**6.27**	**0.9947**	**10.14**	**0.9989**	**11.76**	**1.0002**	**15.62**	**1.0031**	**19.89**	**1.0059**
0.45	0.9845	8.03	0.993	10.34	0.9968	13.56	1.0008	13.46	1.0013	17.43	1.0039	22.09	1.007
1.48	0.9851	11.85	0.995	14.99	0.9993	17.34	1.0028	18.90	1.0043	21.06	1.0059	24.67	1.0083
3.69	0.9863	18.10	0.9983	20.09	1.002	19.62	1.004	22.93	1.0064	24.32	1.0076	28.59	1.0103
7.31	0.9883	28.00	1.0034	27.77	1.0062	27.34	1.008	28.18	1.009	28.13	1.0095		
11.90	0.9907												
19.83	0.9948												
28.62	0.9993												

[a] Density of deionized water without CO_2.

level. The above procedure was repeated until the measurement at the desired lowest saturation pressure was finished.

The maximum uncertainty in pressure measurements is less than ±0.009 MPa. The accuracy of the evolved gas volume measurements (from about 144 cm^3 up to 477 cm^3) is ±1 cm^3 (or the maximum relative uncertainty is 0.7%). The accuracy in the mass measurements of water (from about 10 g up to 30 g) is 0.01 g (or the maximum relative uncertainty is 0.1%). The maximum relative uncertainty for the solubility determined from eq 1 is estimated to be less than 2%. The maximum uncertainty in density measurements is estimated within $\pm 1 \times 10^{-4}$ g·cm^{-3}.

Results and Discussion

In this work, solubilities of CO_2 in deionized water and an oil reservoir formation brine were determined at a temperature of 59 °C and pressures up to 20 MPa. The densities of CO_2 + deionized water and CO_2 + brine solutions were determined as a function of both CO_2 concentration and pressure. The brine sample was collected from the Weyburn reservoir, Saskatchewan, Canada. Its analysis was presented in Table 1. The CO_2 used was supplied by Canadian Liquid Air Ltd. with a purity of 99.99%.

CO_2 Solubility in Deionized Water and Brine. The measured solubilities of CO_2 in deionized water and brine at different pressures are listed in Tables 2 and 3, respectively. These results are presented graphically in Figure 2. The CO_2 solubility vs saturation pressure curves in Figure 2 show that: (1) the solubility of CO_2 in both deionized water and brine increased with pressure; (2) the increase in CO_2 solubility with pressure became less as the pressure increased; (3) the salinity reduced the CO_2 solubility in brine compared with that in deionized water. The CO_2 solubility in Weyburn brine was about 30% lower than that in deionized water at the highest saturation pressure tested.

Several correlations given in the literature[10,15,16] for predicting the solubility of CO_2 in the aqueous phase were examined in this work. The correlation by Chang et al.[15] was found to be more reliable than others when used under reservoir conditions and easier to be applied in reservoir simulation since all the dissolved substances are lumped together as a salinity. This correlation was developed by fitting the experimental data from different researchers.[6,8,9,17]

For CO_2 solubility in water R_w, the correlation of Chang et al.[15] is given as

$$R_w = 1.152^{-3} aP\left[1 - b\sin\left(\frac{\pi}{2}\frac{145cP}{145cP + 1}\right)\right] \quad \text{for} \quad P < P^0/145 \quad (2)$$

$$R_w = 1.152^{-3}[R_w{}^0 + m(145P - P^0)] \quad \text{for} \quad P \geq P^0/145 \quad (3)$$

where the solubility R_w is in mol·cm^{-3}, and P is the total pressure of CO_2 and water in MPa. a, b, c, P^0, $R_w{}^0$, and m are functions of temperature T and they are given as

$$a = \sum_{i=0}^{4} (a_i \times 10^{-3i})\left(\frac{9}{5}T + 32\right)^i \qquad (4)$$

$$b = \sum_{i=0}^{4} (b_i \times 10^{-3i})\left(\frac{9}{5}T + 32\right)^i \qquad (5)$$

$$c = 10^{-3}\sum_{i=0}^{4} (c_i \times 10^{-3i})\left(\frac{9}{5}T + 32\right)^i \qquad (6)$$

$$p^0 = \frac{2}{\pi}\frac{\sin^{-1}(b^2)}{c\left[1 - \frac{2}{\pi}\sin^{-1}(b^2)\right]} \qquad (7)$$

$$R_w{}^0 = ap^0(1 - b^3) \qquad (8)$$

$$m = a\left\{1 - b\left[\sin\left(\frac{\pi}{2}\frac{cp^0}{cp^0 + 1}\right) + \frac{\pi}{2}\frac{cp^0}{(cp^0 + 1)^2}\cos\left(\frac{\pi}{2}\frac{cp^0}{cp^0 + 1}\right)\right]\right\} \qquad (9)$$

where the temperature T is in °C. The forms of eqs 2−6 are different from the original ones given in ref 15 as a result of unit conversion. Values of coefficients a_i, b_i, and c_i in eqs 4−6 are shown in Table 4. For the temperature of 59 °C used in this work, $P^0/145$ was calculated to be 35.5 MPa. Since the maximum pressure of the measurements in this work was lower than 35.5 MPa, eq 2 was used in solubility predictions.

The solubility of CO_2 in brine, R_b, is calculated as[15]

$$R_b = 10^{-\{0.028S\}/\{[(9/5)T+32]^{0.12}\}} R_w \qquad (10)$$

where R_b is in mol·cm^{-3}. S is the salinity of brine, which is defined as the total dissolved salts in the solution in mass percent.[18]

The predicted results from eqs 2 and 10 are also listed in Tables 2 and 3 and plotted in Figure 2. The salinity for Weyburn brine was 8.36 mass %, which was used in eq 10. Comparison between the calculated results and the determined data shows that the Chang et al.[15] correlation can give a satisfactory prediction for CO_2 solubility in both deionized water and formation brine.

Density of Aqueous CO_2 Solution. Measured densities for CO_2 + deionized water and CO_2 + brine solutions are listed in Tables 5 and 6, respectively. In both Tables 5 and 6, the data in the first row (in bold) are the densities at the saturation pressure conditions. The data in the first set of Tables of 5 and 6 are pressures and densities for deionized water and brine, respectively, without dissolution of CO_2. These results are also plotted as a function of pressure for different CO_2 concentrations in Figures 3 and 4, respectively. In these two figures, the curves with solid

Table 6. Densities of CO_2 + Weyburn Brine Solutions at 59 °C

P/MPa	ρ/(g·cm^{-3})[a]	P/MPa	ρ/(g·cm^{-3})	P/MPa	ρ/(g·cm^{-3})	P/MPa	ρ/(g·cm^{-3})	P/MPa	ρ/(g·cm^{-3})	P/MPa	ρ/(g·cm^{-3})	P/MPa	ρ/(g·cm^{-3})
		1.76	**1.0484**	**3.01**	**1.0497**	**6.20**	**1.0534**	**10.38**	**1.0562**	**15.73**	**1.0596**	**20.87**	**1.0628**
0.24	1.046	6.58	1.0507	10.54	1.0534	10.14	1.0555	14.29	1.0581	18.96	1.0613	24.38	1.0646
0.83	1.0463	15.17	1.055	14.14	1.0552	13.89	1.0574	17.55	1.0599	20.83	1.0624	25.96	1.0655
2.27	1.0471	22.85	1.0588	22.03	1.0591	20.86	1.0609	21.84	1.0621	24.27	1.0642	27.69	1.0666
6.32	1.0491	28.64	1.0616	28.64	1.0623	28.46	1.0648	27.83	1.0651	27.62	1.066		
10.79	1.0513												
18.67	1.0552												
24.52	1.058												
28.93	1.0601												

[a] Density of Weyburn brine without CO_2.

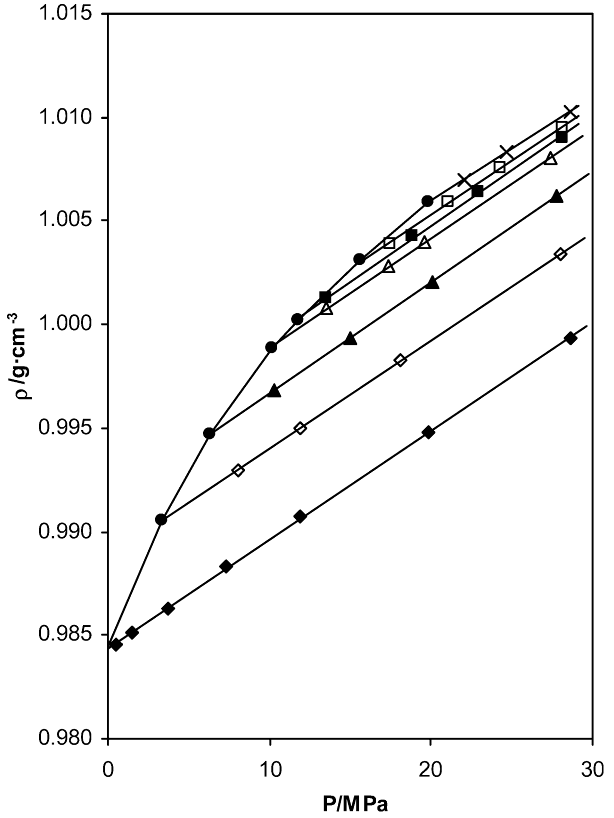

Figure 3. Density of CO_2 + deionized water solution vs pressure with different CO_2 concentrations at 59 °C. ◆, deionized water, $C = 0$; ◇, $C = 0.514 \times 10^{-3}$ mol·cm^{-3}; ▲, $C = 0.835 \times 10^{-3}$ mol·cm^{-3}; △, $C = 1.089 \times 10^{-3}$ mol·cm^{-3}; ■, $C = 1.127 \times 10^{-3}$ mol·cm^{-3}; □, $C = 1.227 \times 10^{-3}$ mol·cm^{-3}; ×, $C = 1.344 \times 10^{-3}$ mol·cm^{-3}; ●, at different saturation pressures.

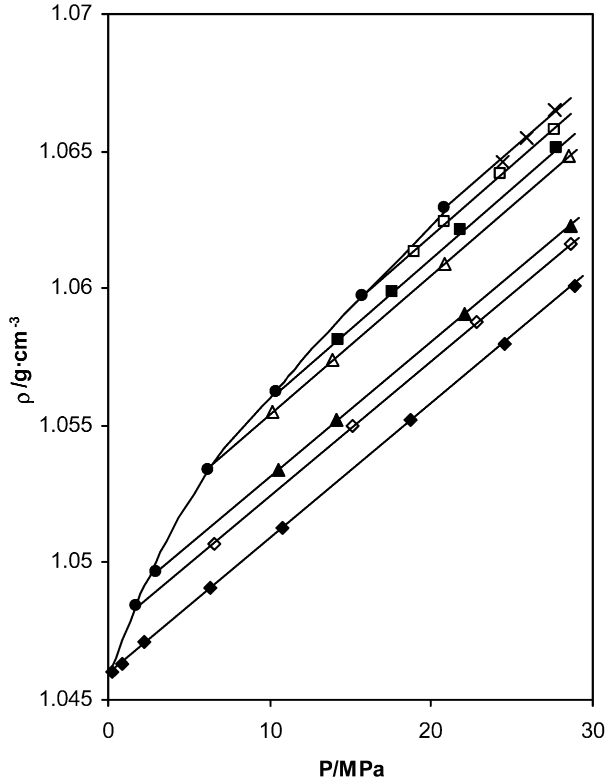

Figure 4. Density of CO_2 + Weyburn brine solution vs pressure with different CO_2 concentrations at 59 °C. ◆, Weyburn brine, $C = 0$; ◇, $C = 0.24 \times 10^{-3}$ mol·cm^{-3}; ▲, $C = 0.367 \times 10^{-3}$ mol·cm^{-3}; △, $C = 0.626 \times 10^{-3}$ mol·cm^{-3}; ■, $C = 0.814 \times 10^{-3}$ mol·cm^{-3}; □, $C = 0.905 \times 10^{-3}$ mol·cm^{-3}; ×, $C = 0.958 \times 10^{-3}$ mol·cm^{-3}; ●, at different saturation pressures.

diamonds represent the densities of the aqueous phase without CO_2 (or at zero CO_2 concentration), the curves with solid circles represent the densities of CO_2 saturated aqueous solutions at different saturation pressures, and the rest of the curves represent the densities of unsaturated solutions at different CO_2 concentrations, C.

As shown in Figures 3 and 4, for a given CO_2 concentration, the density of the solution for both deionized water and brine increased linearly with pressure. All these curves had the same slope as that of the aqueous phase at zero CO_2 concentration within experimental errors. For a constant pressure, the density of aqueous solution increased with CO_2 concentration. In other words, the dissolution of CO_2 in both deionized water and brine increased the density of the aqueous phase.

In Figures 5 and 6, the density of aqueous CO_2 solutions at selected pressures was plotted as a function of CO_2 concentration for the CO_2 + deionized water and CO_2 + brine systems, respectively. In these two figures, the intercept of each curve represents the density of the aqueous phase with zero CO_2 concentration, and the end point of each curve represents the density of CO_2 saturated aqueous solution at the corresponding pressure. These results indicated that the density of aqueous CO_2 solution at a given pressure increased linearly with CO_2 concentration for both CO_2 + deionized water and CO_2 + brine systems. In each system, all the curves of different pressures had the same slope, β, within the experimental errors. The slope for CO_2 + deionized water ($\beta = 8.456$ g·mol^{-1}) was a bit higher than that for CO_2 + brine ($\beta = 6.738$ g·mol^{-1}). Similarly, Ohsumi et al.[2] observed a linear relationship between the density increase and CO_2 concentration in their measurements for CO_2 + seawater. On the basis of the relationship shown in Figures 5 and 6, the density of aqueous CO_2 solutions can be calculated by

$$\rho/(\mathrm{g \cdot cm^{-3}}) = \rho_p/(\mathrm{g \cdot cm^{-3}}) + \beta/(\mathrm{g \cdot mol^{-1}})C/(\mathrm{mol \cdot cm^{-3}}) \qquad 0 \le C \le C_{sat} \quad (11)$$

where ρ_p is the density of the aqueous phase with zero CO_2

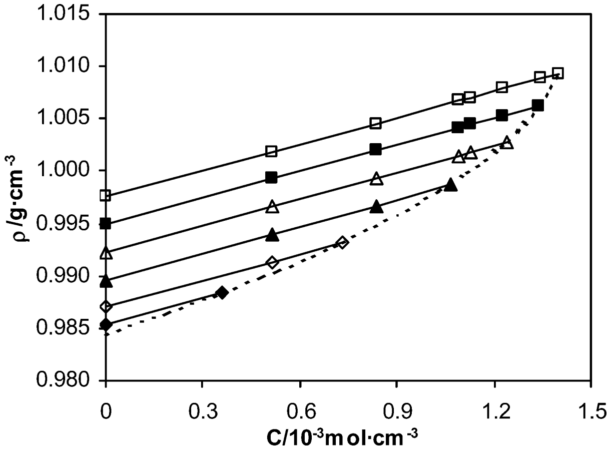

Figure 5. Density of CO_2 + deionized water vs CO_2 concentration under selected pressures at 59 °C. ◆, 2 MPa; ◇, 5 MPa; ▲, 10 MPa; △, 15 MPa; ■, 20 MPa; □, 25 MPa.

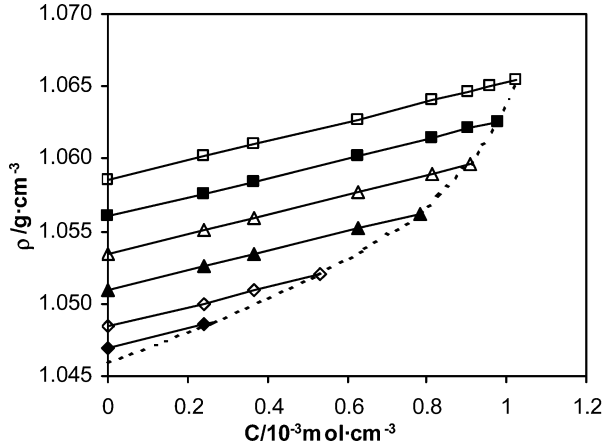

Figure 6. Density of CO_2 + Weyburn brine vs CO_2 concentration under selected pressures at 59 °C. ◆, 2 MPa; ◇, 5 MPa; ▲, 10 MPa; △, 15 MPa; ■, 20 MPa; □, 25 MPa.

Table 7. Values of Parameters in Equations 11 and 12

	β/(g·mol^{-1})	α/(10^{-4} g·cm^{-3}·MPa^{-1})	ρ_0/(g·cm^{-3})
deionized water	8.456	5.241	0.9844
Weyburn brine	6.738	5.045	1.0459

concentration at given pressure *P*. *C* is the concentration of CO_2 in aqueous solution, C_{sat} is the CO_2 solubility in aqueous solution at the corresponding pressure *P*, ρ is the density of CO_2 aqueous solutions at CO_2 concentration *C* and pressure *P*, and β is the slope of density vs concentration in Figures 5 and 6. ρ_p is determined by

$$\rho_p = \rho_0 + \alpha P \qquad (12)$$

where *P* is the pressure and α is the slope of density vs pressure with zero CO_2 concentration for deionized water or brine, i.e., the slope of the curve with solids diamonds in Figure 3 for CO_2 + deionized water and that in Figure 4 for CO_2 + brine. ρ_0 is the intercept of the curve of density vs pressure at zero CO_2 concentration in Figures 3 and 4 for deionized water and brine, respectively. Values of β, α, and ρ_0 for the systems tested in this work are listed in Table 7.

Three parameters β, α, and ρ_0 in eqs 11 and 12 may change with the water samples (such as brine at different salinities) and temperature. A simple method for determining the density of aqueous CO_2 solutions can be proposed as follows. The first step is to measure the density of the aqueous phase with zero CO_2 concentration as a function of pressure to find ρ_0 and α in eq 12. The second step is to measure densities of aqueous CO_2 solution at a constant pressure but different CO_2 concentrations to find the value of β. Then apply eqs 11 and 12 for the same CO_2 + water system to calculate the density of aqueous CO_2 solution as a function of CO_2 concentration and pressure at a constant temperature.

Conclusions and Recommendations

Solubilities of CO_2 in deionized water and brine and densities of CO_2 + deionized water and CO_2 + brine solutions were measured at a temperature of 59 °C and pressures up to 29 MPa. It was found that: (1) The dissolution of CO_2 in both deionized water and brine increases the density of aqueous phase. (2) For a constant CO_2 concentration, the density of an aqueous CO_2 solution increases linearly with pressure. For the same CO_2−aqueous system and at a constant temperature, the slopes of density vs pressure curves for different CO_2 concentrations are the same. (3) Similarly, for a constant pressure, the density of an aqueous CO_2 solution increases linearly with CO_2 concentration. For the same CO_2−aqueous system and at a constant temperature, the slopes of density vs concentration curves for different pressures are the same. (4) The Chang et al.[15] correlation can provide a good prediction for CO_2 solubility in the deionized water and brine.

A correlation for density of aqueous CO_2 solutions was presented based on the results of this work. A simple method for determining the density of aqueous CO_2 solutions was recommended.

Literature Cited

(1) Haugan, P. M.; Drange, H. Sequestration of CO_2 in the Deep Ocean by Shallow Injection. *Nature* **1992**, *357*, 318−320.

(2) Ohsumi T.; Nakashiki N.; Shitashima K.; Hirama K. Density Change of Water due to Dissolution of Carbon Dioxide and Near-Field Behavior of CO_2 from a Source on Deep-sea Floor. *Energy Convers. Manage.* **1992**, *33*, 685−690.

(3) Teng, H.; Yamasaki A.; Chun, M.-K.; Lee, H. Solubility of Liquid CO_2 in Water at Temperatures from 278 K to 293 K and Pressures from 6.44 MPa to 29.49 MPa and Densities of the Corresponding Aqueous Solutions. *J. Chem. Thermodyn.* **1997**, *29*, 1301−1310.

(4) Parkinson, W. J.; Nevers, N. D. Partial Molal Volume of Carbon Dioxide in Water Solutions. *Ind. Eng. Chem. Fundam.* **1969**, *8*, 709−713.

(5) Yaginuma R.; Sato, Y.; Kodama, D.; Tanaka, H.; Kato, M. Saturated Densities of Carbon Dioxide + Water Mixture at 304.1 K and Pressures up to 10 MPa. *Nihon Enerugi Gakkaishi* **2000**, *79*, 144−146.

(6) Wiebe, R. The Binary System Carbon Dioxide-Water under Pressure. *Chem. Rev.* **1941**, *29*, 475−481.

(7) Steward, P. B.; Munjal P. Solubility of Carbon Dioxide in Pure Water, Synthetic Seawater, and Synthetic Seawater Concentrates at −5° to 25 °C and 10 to 45 Atm. Pressure. *J. Chem. Eng. Data* **1970**, *15*, 67−71.

(8) Malinin, S. D.; Savelyeva, N. I. The Solubility of CO_2 in NaCl and $CaCl_2$ Solutions at 25, 50, and 75° under Elevated CO_2 Pressures. *Geochemistry International* **1972**, *9*, 410−418.

(9) Malinin, S. D.; Kurovskaya, N. A. Solubility of CO_2 in Chloride Solutions at Elevated Temperatures and CO_2 Pressures. *Geochem. Int.* **1975**, *12*, 199−201.

(10) Nighswander, J. A.; Kalogerakis, N.; Mehrotra, A. K. Solubility of Carbon Dioxide in Water and 1 wt % NaCl Solution at Pressures up to 10 MPa and Temperatures from 80 to 200 °C. *J. Chem. Eng. Data* **1989**, *34*, 355−360.

(11) Rumpf, B.; Maurer, G. An Experimental and Theoretical Investigation on the Solubility of Carbon Dioxide in Aqueous Solutions of Strong Electrolytes. *Ber. Bunsen−Ges. Phys. Chem.* **1993**, *97*, 85−97.

(12) Rumpf, B.; Xia, J.; Maurer, G. Solubility of Carbon Dioxide in Aqueous Solutions Containing Acetic Acid or Sodium Hydroxide in the Temperature Range from 313 to 433 K and at Total Pressures up to 10 MPa. *Ind. Eng. Chem. Res.* **1998**, *37*, 2012−2019.

(13) Xia, J.; Rumpf, B.; Maurer, G. Solubility of Carbon Dioxide in Aqueous Solutions Containing Sodium Acetate or Ammonium Acetate at Temperatures from 313 to 433 K and Pressures up to 10 MPa. *Fluid Phase Equilib.* **1999**, *155*, 107−125.

(14) Kamps, A. P.; Balaban, A.; Jodecke, M.; Kuranov, G., Smirnova, N. A.; Maurer, G. Solubility of Single Gases Carbon Dioxide and Hydrogen Sulfide in Aqueous Solutions of *N*-Methyldiethanolamine at Temperatures from 313 to 393 K and Pressures up to 7.6 MPa: New Experimental Data and Model Extension. *Ind. Eng. Chem. Res.* **2001**, *40*, 696−706.

(15) Chang, Y. B.; Coats, B. K.; Nolen, J. S. A Compositional Model for CO_2 Floods Including CO_2 Solubility in Water. *SPE Reservoir Eval. Eng.* **1998**, *April*, 155−160.

(16) Li, Y.-K.; Nghiem, L. X. Phase Equilibria of Oil, Gas and Water/Brine Mixtures form a Cubic Equation of State and Henry's Law. *Can. J. Chem. Eng.* **1986**, *64*, 486-496.

(17) McRee, B. C. CO_2: How It Works, Where It Works. *Pet. Eng.* **1977**, *49*, 52−63.

(18) Norman, J. H. *Dictionary of Petroleum Exploration, Drilling & Production*; PennWell Publishing Company: Tulsa, Oklahoma, 1991.

Received for review February 3, 2004. Accepted April 29, 2004. The financial support by the Petroleum Technology Research Center (PTRC), Regina, Saskatchewan is gratefully acknowledged.

JE049945C